Steel and Composite Structures, *Vol. 19*, *No. 1* (*2015*) *209-221*
DOI: http://dx.doi.org/10.12989/scs.2015.19.1.209

Experimental research on seismic behavior of novel composite RCS joints

Jinjie Men [*], Zhifeng Guo [a] and Qingxuan Shi [b]

College of Civil Engineering, *Xi'an University of Architecture & Technology*, *13 Yanta Road*, *Xi'an*, *Shaanxi Province*, *710055*, *China*

(*Received May 21*, *2014*, *Revised December 17*, *2014*, *Accepted December 30*, *2014*)

Abstract. Results from an experimental study on the seismic response of six composite reinforced concrete column-to-steel beam interior joints are presented. The primary variable investigated is the details in the joint. For the basic specimen, the main subassemblies of the beam and column are both continuous, and the steel beam flanges extended to the joint are partly cut off. Transverse beam, steel band plates, cove plates, X shape reinforcement bars and end plates are used in the other five specimens, respectively. After the joint steel panel yielded, two failure modes were observed during the test: local failure in Specimens 1, 2 and 4, shear failure in Specimens 3, 5 and 6. Specimens 6, 3, 5 and 4 have a better strength and deformation capacity than the other two specimens for the effectiveness of their subassemblies. For Specimens 2 and 4, though the performance of strength degradation and stiffness degradation are not as good as the other four specimens, they all have excellent energy dissipation capacity comparing to the RC joint, or the Steel Reinforced Concrete (SRC) joint. Based on the test result, some suggestions are presented for the design of composite RCS joint.

Keywords: composite structure; joint details; earthquake resistant structures; seismic behavior; capacity; shear failure

1. Introduction

Composite frame systems consisting of Reinforced Concrete columns and structural Steel beams (RCS) have gained increasing interest in the past 30 years due to their cost-and time-effective behaviors (Griffis 1986). Many kinds of details on composite RCS joints were proposed in the US, Japan and China (Hiroshi and Isao 2004, Deierlein and Noguchi 2004, Guo *et al*. 2012), and many experimental studies have been conducted to make sure of seismic performance of the joint (Sheikh *et al*. 1989, Miehael *et al*. 2000, Fargier-Gabaldón and Parra-Montesinos 2006, Chou and Wu 2007, Chou *et al*. 2008). The above test results showed that RCS joints exhibit excellent performance when subjected to large inelastic deformations. In 1994, ASCE published design guidelines for composite RCS joints in low to moderate seismic regions

*Corresponding author, Professor, E-mail: menjinjie@yahoo.com
[a] Ph.D. Student, E-mail: guozhifeng2007@126.com
[b] Professor, E-mail: shi_qx@126.com

http://www.techno-press.org/?journal=scs&subpage=8 ISSN: 1229-9367 (Print), 1598-6233 (Online)

(ASCE 1994). And more recently, research work has been focused on the development of design guidelines for composite connections in RCS frame structures located in zones of high seismicity (Liang and Parra-Moniesinos 2004, Bahman *et al*. 2013). Furthermore, results from pseudo-dynamic tests of RCS moment frame (Chen *et al*. 2004, Cordova *et al*. 2004, Chou and Chen 2010) demonstrated the suitability of RCS frame construction for use in zones of high seismicity.

The research work presented in this paper focuses on a novel composite RCS joint. For this kind joint, the main component of the beam and column are both continuous. The steel beam web passes continuous through the joint, thereby avoiding interruption of the beam entirely at the column face. The steel beam flanges extend into the joint and are partly cut off, which can keep the longitudinal reinforcement of the column passing through the joint and facilitate casting and vibrating the concrete. The joint details are shown in Fig. 1 and will be described in Section 2.1.

To promote the use of the novel RCS joints, besides the advantage of the details described above, the mechanical behavior of the joints also should be clarified. The objective of the

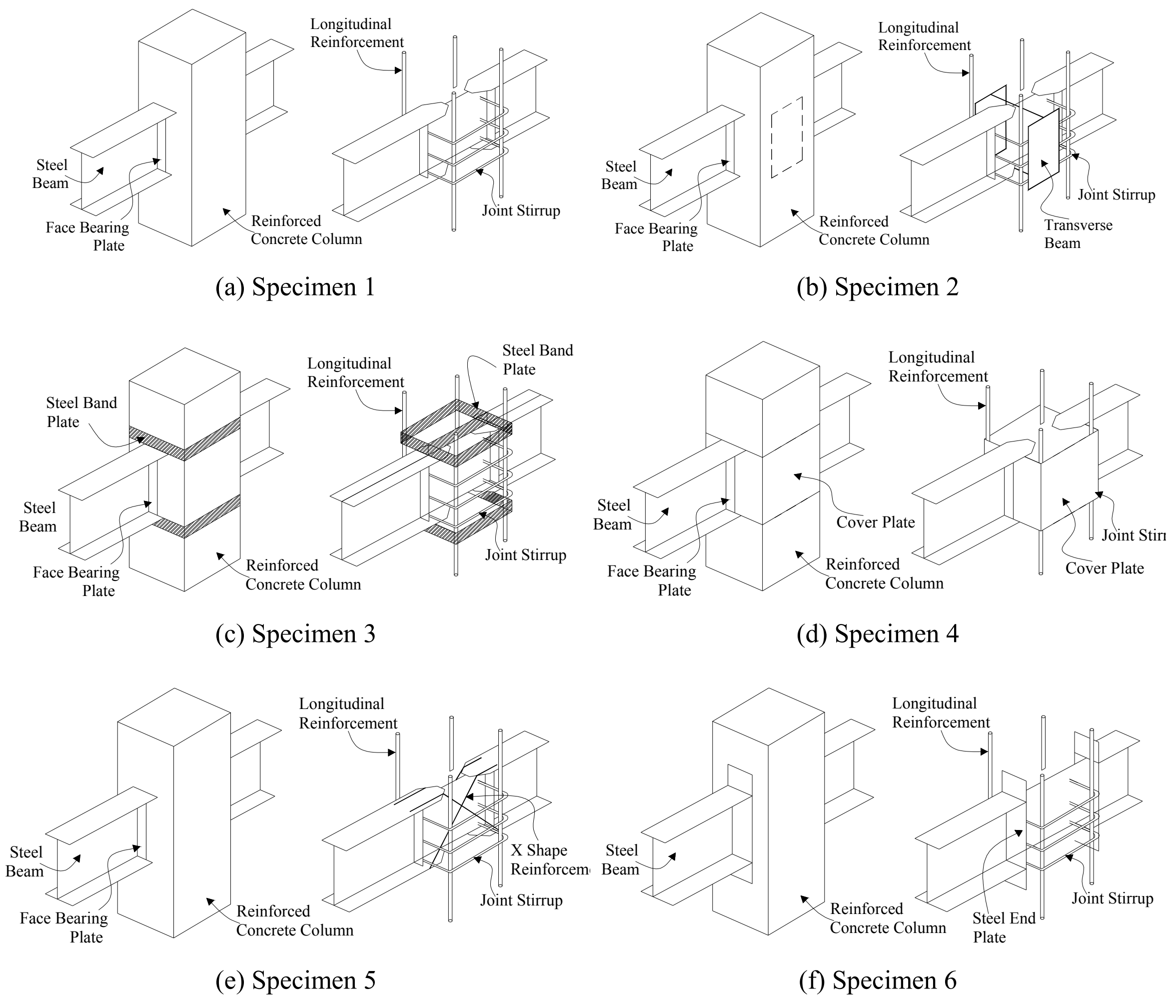

Fig. 1 Details of the specimen

current research program is to evaluate the design, constructability, and seismic performance of the composite RCS joints. Test results are presented here in terms of cracking, yielding and failure mode, strength and deformation capacity, strength and stiffness degradation, and energy dissipation capacity. The design suggestion for the composite RCS joints are also presented in the paper.

2. Experimental program

2.1 Description of test specimens

The experimental program involved the testing of six approximately 1/2-scale interior RCS connections subjected to cyclic lateral loading. The RC columns had a length of 2550 mm and a 350 mm square cross section. Column longitudinal reinforcement included twelve 20 mm deformed bars, representing approximately 3.08% of the column gross area. HN350×175×7×11 shape steel were used for the 2250 mm long steel beams.

It should be emphasized that the specimens were designed such that the connection represented the weakest link of the subassembly. Therefore, most of the inelastic activity would concentrate in the joint region, allowing the evaluation of the inelastic response of RCS joints when subjected to severe earthquake loading.

Specimen 1 was designed and used as a base for comparison to the other five specimens. In Specimen 1, the steel beam flanges extends to the joint and are partly cut off, which can keep the longitudinal reinforcement of the column passing through the joint and facilitate casting and vibrating the concrete. Face bearing plates (FBP) were fillet welded to the beam flanges at the front and back faces of the columns. A ratio of stirrup volume to joint volume of approximately 0.61% was used, consisting of five layers of overlapping 8 mm U-shaped hoops passing through the web of the steel beam. Fig. 1(a) shows the joint details used in Specimen 1.

Specimen 2 has the same joint details as Specimen 1, but a transverse beam was welded to the beam web by web orthogonally. In Specimen 3, steel band plate was welded to the top and the bottom of the beam, which has the same external size of the column. In Specimen 4, the stirrup was replaced by a cover plate. And in Specimen 5, two X shape reinforcement bars were welded to the flange of the beam. In Specimen 6, the steel beam was bolted to the flanges of an H shape steel, through beam end plates. And five layers of U-shaped hoops were used passing through the web of the H shape steel. The joint details of Specimen 2-6 were shown in Figs. 1(b)-(f), respectively, and their features were described in Table 1.

The construction and loading of this test frame was carried out in Key Laboratory of Structural Engineering and Seismic Resistance, Ministry of Education, in Xi'an. The steel beam and the subassembly of the joint were processed and made in the machine shop. Then the longitudinal reinforcement and stirrups of the column were assembled and the concrete was casted in the lab.

2.2 Material properties

Grade HRB335 deformed steel bars were used for all the reinforcement in the columns and the X shape rebar for Specimen 5. And Grade Q235 steel was used for all the shape steel, FBPs and other steel plates. The material properties of the reinforcement and the steel are got based on three coupons for each reinforcement bar or steel plate. The yield tensile strength (f_y) and the ultimate

Table 1 Description of test specimens

Specimen number	Features
1	HN350×175 beam with FBP, five stirrups (d = 8 mm) in joint
2	HN350×175 beam with FBP, transverse beam (HN350×175), five stirrups (d = 8 mm)in joint
3	HN350×175 beam with FBP, steel band plate (t = 6 mm), five stirrups (d = 8 mm) in joint
4	HN350×175 beam with FBP, cover plate(t = 4 mm), no stirrup in joint
5	HN350×175 beam with FBP, X rebar (d = 12 mm), five stirrups (d = 8 mm) in joint
6	Built-up beam with end plate (t = 20 mm), H shape steel (HN350×175) and five stirrups (d = 8 mm) in joint

*Note: t = thickness; d = diameter; the thickness of all FBP is 10 mm
HN350×175 represents HN350×175×7×11 shape steel

Table 2 Material properties

Components	t or d/mm	f_y /MPa	f_u /MPa	E_s /MPa	ε_y /$\mu\varepsilon$
Beam flange	11	287.7	448.4	1.99×10^5	1445
Beam web	7	308.5	445.0	1.84×10^5	1676
Face bearing plates	10	317.0	437.4	2.02×10^5	1569
Cover plates	4	289.8	396.5	1.84×10^5	1575
Steel band plates	6	358.2	445.2	2.11×10^5	1697
Reinforced bar	8	500.0	685.0	2.15×10^5	2325
Reinforced bar	12	395.0	575.0	1.97×10^5	2005
Reinforced bar	20	330.0	540.0	2.03×10^5	1625

*Note: t = thickness; d = diameter; $\mu\varepsilon = \Delta L/L\times10^{-6}$

tensile strengths (f_u) of the reinforcement and the steel, also with the elastic modulus (E_s) and yielding strain (ε_y), are listed in Table 2. The concrete design strength grade is C60. And the concrete compressive strengths for the columns at test day are 64.47 Mpa, which also are obtained based on three cubes for each concrete pour.

2.3 Test setup, load and displacement history and instruments

The test setup used for the experimental program is shown in Fig. 2. The columns and the steel beam are pinned at their ends. The pins represent the inflection points that are likely to occur at column mid-height and beam mid-span during a seismic event. The pin at the ends of the beam were supported by two vertical steel links that allowed horizontal displacements but restrained vertical movements, while the pin at the bottom column end restrained both vertical and horizontal displacements. Axial compression load was applied to the columns through a hydraulic jack, which is determined by the design axial compression ratio of 0.3. Then lateral reversed-cyclic displacements were applied at the top of the column through a 500 kN hydraulic actuator. The load and displacement history includes two stage: elastic cycle and inelastic cycle. Before yielding, load cycles were applied to the specimen, which increased by 10kN in each elastic cycle. After

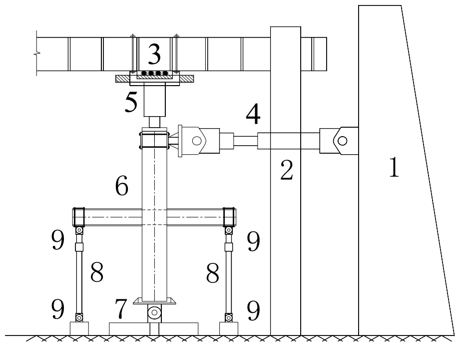

1. Reaction wall; 2. Rigid frame; 3. Rigid beam; 4. Hydraulic actuator;
5. Hydraulic jack; 6. Specimen; 7. Column pins; 8. Force transducers; 9. Beam pins

Fig. 2 Experiment equipments

yielding, displacement cycles were applied to the specimens, with displacement increases by Δ_y (a scale of the yielding displacement). Each displacement cycle was repeated twice to study the stiffness and strength deterioration at that drift level. When the lateral load reduced to about 85% of the peak load, the test was stopped.

A load cell and a displacement transducer were used to monitor the applied lateral load and displacement at the top of the column. Three displacement transducers were also placed near the two end of the beam to monitor the vertical and the lateral displacement. Linear potentiometers and clinometers were used to measure joint deformations and beam rotations. Strains in the steel beam web and flanges, band plates, cover plates, X shape rebar and in the column reinforcement, were monitored through linear and rosette strain gauges.

3. Specimen behavior

3.1 Cracking, yielding and failure modes

Two typical cracking modes were observed for the six specimens. For Specimens 1, 2 and 4 (Group 1), the initial crack occurred on the column surface perpendicular to the beam, which extended from the beam flange to the column edge. Vertical cracks also were observed on the joint surface in Specimen 1 and 2, which is closed to the column edge in the later test stage. For these three specimens, there is no diagonal crack on the surface of the joint area parallel to the beam. For Specimens 3, 5 and 6 (Group 2), the initial crack still occurred and developed in the same place and the same way, but diagonal cracks were observed obviously on the surface of the joint area parallel to the beam.

For all the specimens, the joint steel panel yielded first and earlier than the other joint details. At the last loading cycle, the strain of the joint steel panel is about 2,247 $\mu\varepsilon$ to 2,709 $\mu\varepsilon$. While the maximum strain of the beam flange and the column longitudinal reinforcement is about 906 $\mu\varepsilon$ to 940 $\mu\varepsilon$ and 358 $\mu\varepsilon$ to 458 $\mu\varepsilon$, respectively. That means the connection represents the weakest link of the subassembly which is expected to occur by the objective of the research. At the fifth displacement cycle, the other joint details also became into yielding. For example, the steel beam

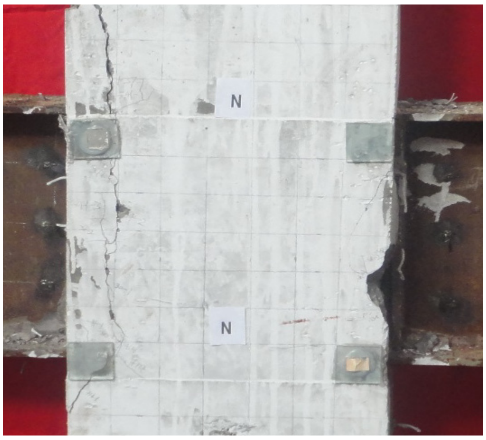

(a) Specimen 1

(b) Specimen 2

(c) Specimen 3

(d) Specimen 4

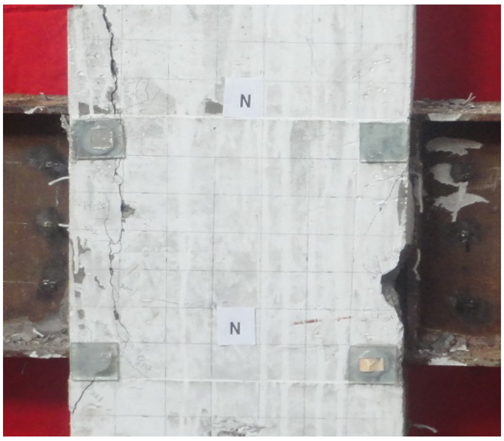

(e) Specimen 5

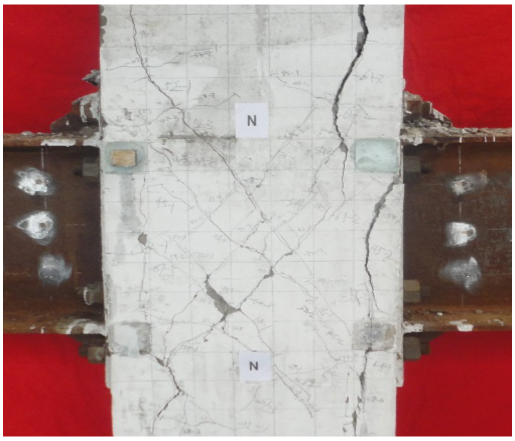

(f) Specimen 6

Fig. 3 Failure photos of the specimen

flange were local bulked in Specimen 1, the band plate, the cover plate and the X shape reinforcement yielded in Specimen 3, 4 and 5, respectively. The yielding of the above joint details indicates that the design and the constructability of the specimen are suitable for the RCS connection, for they can take their effect under the lateral reversed-cyclic load.

At the end of the test, the failure mode of the six specimen can be classified to two types. For Specimens 1, 2 and 4, the concrete were crushed out mainly in two areas: at the end of the column just on and under the beam flange, and in the inner area of the joint just between the beam flanges. For Specimens 3, 5 and 6, besides the concrete were crushed out at the end of the column and in the inner area of the joint, the concrete in the outer area of the joint were also damaged caused by shear stress. The failure photos of all the specimens are shown in Fig. 3.

3.2 Strength and lateral displacement

Experimental results on the strength and the displacement are shown in Table 3. P_{cr}, P_y, $P_{\max}$ and P_u represent the cracking strength, yielding strength, peak strength and the ultimate strength, respectively. Δ_{cr}, Δ_y, $\Delta_{\max}$, Δ_u and θ_{cr}, θ_y, $\theta_{\max}$, θ_u are the corresponding displacement and inter-story drift ratio. Table 3 shows that the strength of Specimen 1 and 2 are almost the same, which means the transverses beam nearly has no effect on the capacity. The strength of the other four specimens are much larger than Specimen 1.The order from high to low is Specimen 6, 3, 5 and 4. And the rate increased in yielding strength and peak strength are about 48%, 43%, 28%, 22% and 34%, 26%, 14%, 8%, respectively. This significant increase is attributed to the effectiveness of the joint details. The end plates and the wide FBPs in Specimen 6 extend the area of the inner concrete to transfer shear forces. The band plates above and below the joint in Specimen 3 can help transferring shear forces and confining the concrete regions outside the width of the beam flanges, which maintained the integrity of the connection and prevented spalling of the concrete in the corners of the joint. The increase in Specimen 5 is attributed to the X shape reinforcement to

Table 3 Experimental results on the strength and the displacement

Specimens number	P_{cr} /kN	Δ_{cr} /mm	θ_{cr} /rad	P_y /kN	Δ_y /mm	θ_y /rad	$P_{\max}$ /kN	$\Delta_{\max}$ /mm	$\theta_{\max}$ /rad	P_u /kN	Δ_u /mm	θ_u /rad	μ
1	80.3	8.4	1/303	120.2	15.5	1/165	147.3	28.1	1/91	125.2	51.9	1/49	3.3
	-81.0	-13.0	1/196	-110.0	-21.3	1/120	-148.2	-44.2	1/58	-126.0	-59.7	1/42	2.8
2	119.3	19.0	1/134	120.4	19.7	1/129	142.3	46.8	1/54	120.9	55.2	1/46	2.8
	-119.6	-23.0	1/111	-134.6	-27.6	1/92	-163.2	-46.6	1/54	-138.7	-56.1	1/45	2.0
3	149.8	20.7	1/123	163.2	25.1	1/101	186.5	58.8	1/43	175.8	108.4	1/23	4.3
	-149.6	-28.8	1/88	-165.5	-33.6	1/76	-186.4	-66.3	1/38	-176.8	-120.0	1/21	3.6
4	79.2	9.1	1/280	138.5	22.2	1/115	157.0	43.3	1/58	133.4	54.9	1/46	2.5
	-79.9	-19.1	1/133	-141.3	-33.3	1/76	-161.7	-53.2	1/47	-137.4	-73.1	1/35	2.2
5	89.7	10.8	1/236	152.0	23.1	1/110	171.1	33.0	1/77	145.5	58.6	1/44	2.5
	-90.0	-15.7	1/162	-143.1	-29.5	1/86	-165.5	-43.0	1/59	-143.8	-87.6	1/29	3.0
6	90.2	7.9	1/324	165.5	24.0	1/106	192.5	47.8	1/53	169.8	78.4	1/33	3.3
	-89.9	14.2	1/180	-175.0	-33.2	1/77	-204.8	-72.3	1/35	-188.7	-94.5	1/27	2.8

transfer shear force effectively. And it is a simple way for enhancing the joint capacity. Though the increase in Specimen 4 is not so large, cover plates is still an effective measure to confine the concrete inside it.

It is found from Table 3, comparing to Specimen 1, the deformation capacity of the other five specimens were strongly increased. The rate increased in yielding displacement and ultimate displacement for Specimen 2-6 are about 28%, 59%, 50%, 42% 55% and 0%, 104%, 14%, 31%, 54% respectively. Especially for Specimens 6 and 3, the ultimate displacement is about 1.5 and 2.0

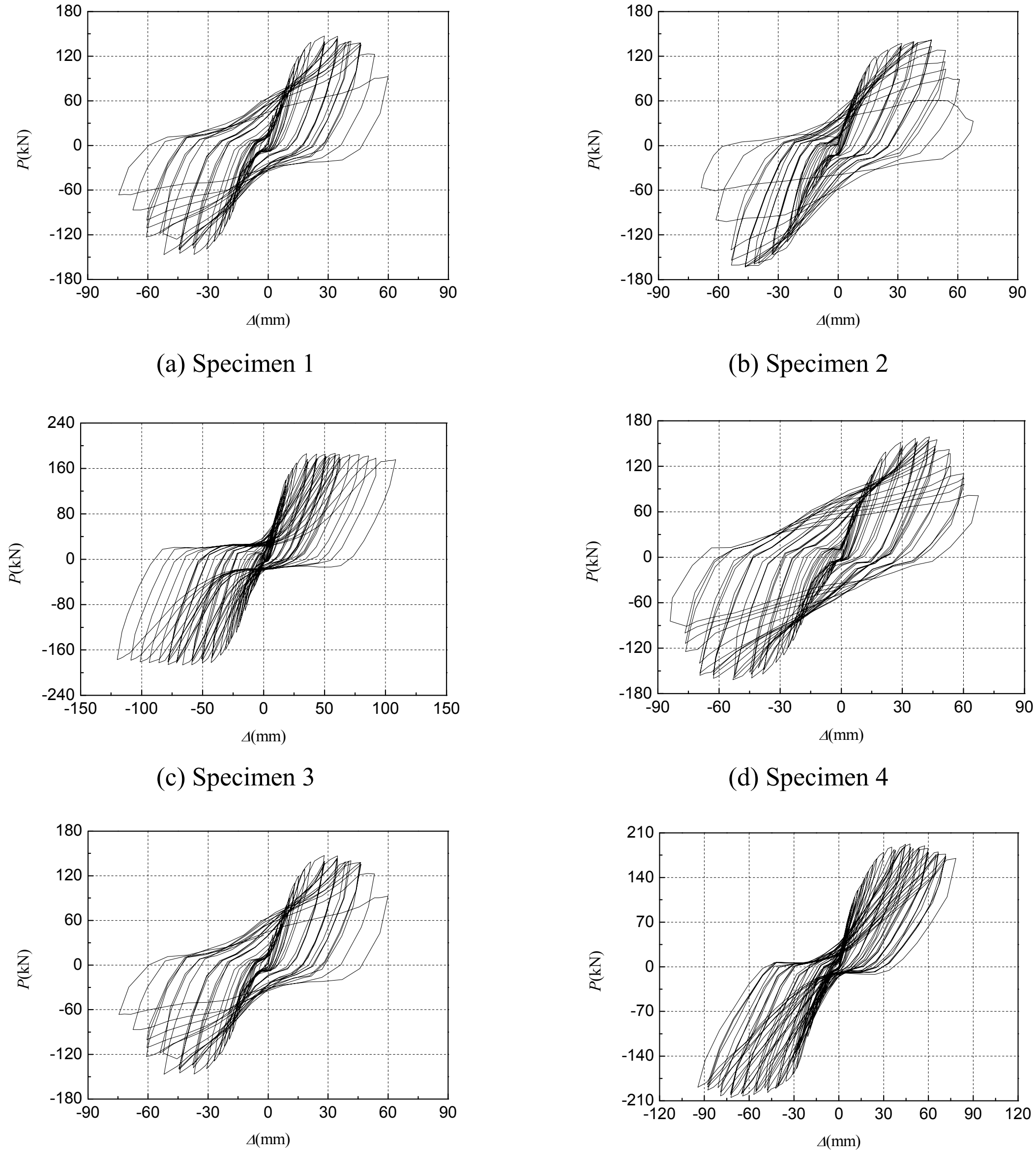

(a) Specimen 1 (b) Specimen 2

(c) Specimen 3 (d) Specimen 4

(e) Specimen 5 (f) Specimen 6

Fig. 4 *P*-Δ hysteretic curves of the specimen

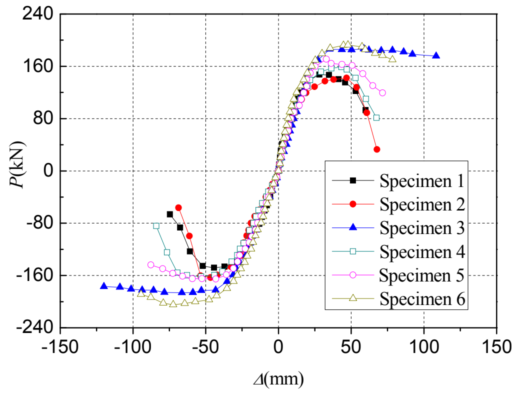

Fig. 5 Skeleton curves of the specimen

times of Specimen 1. It is because that the details in the joint not only can transfer the shear force but also can confine the concrete in the joint effectively, especially when the RCS joint subjected to severe action. Table 3 also shows that the displacement ductility coefficient of each specimen is larger than 2.0 and the average value of the six specimens is 2.9, which is enough to meet the deformation requirement for earthquake resistant structures, even the joint failed earlier than the beam or the column when subjected to severe earthquake loading.

3.3 Hysteretic curves

Load versus displacement (P-Δ) hysteretic curves of the six specimens are shown in Fig. 4. It can be seen that the hysteresis loops of the three specimens in Group 1 are plump with a bow shape, and symmetrical in the two loading directions. While the other three specimens in Group 2 have an inverse "S" shape. For the specimens in Group 1, slight pinching can be noticed in the hysteretic loops in the early stage, primarily due to the cracking at the column end close to the beam flange. However, at larger displacement cycles, during which large joint shear deformations occurred, full hysteresis loops were observed that led to good energy dissipation capacity. For the specimens in Group 2, there is almost no residual deformation at early loading cycle although cracking of the concrete were observed at the end of the column. At larger displacement cycles, the residual deformation is still very small and the hysteresis loops was full, which led to excellent energy dissipation capacity. This is attributed to the effectiveness of the joint details. It should be noticed that all the hysteresis loops are stable even at the fourth displacement cycle. Especially for Specimen 3, the hysteresis loops keep on full and have a strong trend for deformation capacity. It is because that the band plate extend the joint concrete and enhance the integrity of the connection. The difference of the hysteretic curves for the six specimens indicates that the joint details have much effect on the seismic behavior of RCS joints. Generally, a joint with full hysteresis loop means it will present a good seismic behavior.

3.5 Strength degradation

The strength degradation is measured by a strength degradation coefficient λ, which is defined as $\lambda_j = Q_{j3,\max}/Q_{j1,\max}$ where $Q_{j3,\max}$ is the peak load of the third cycle at $j\Delta_y$ displacement, and $Q_{j1,\max}$ is peak load of the first cycle at $j\Delta_y$ displacement. The λ versus Δ/Δ_y curves of the six specimens

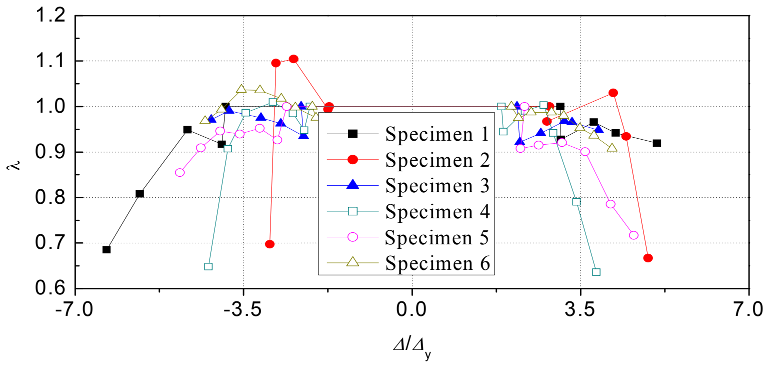

Fig. 6 Strength degradation of the specimen

are shown in Fig. 6. From Fig. 6 it can be seen that for Specimen 2 and 4, λ decreases suddenly at $+4\Delta_y$, $+3\Delta_y$ and $-2\Delta_y$, $-3\Delta_y$, which is mainly because the crush of concrete under the beam flange and the bulk of the cover plate at the above displacement, respectively. The curve of the strength degradation coefficients of the other specimen are relatively smooth, which indicate the cracking of concrete and the yielding of the joint detail are more gentle and complete than the two specimen. It can also be seen that the strength degradation coefficient of Specimen 6 is a little larger than that of the others in general. These phenomena indicate that strength degradation can be slowed down and the seismic performance of the RCS joint can be improved by proper joint details.

3.6 Stiffness degradation

The stiffness degradation herein refers to the decrease of secant stiffness of the joint with the increasing repeated cycles and displacement. The secant stiffness of the six specimens are plotted in Fig. 7. It is shown that the stiffness degradation started from the beginning of the test. And the initial stiffness under the reverse lateral load is smaller than that under the forward lateral load. It is because that there are always gaps between the test setups though they are fixed as much as

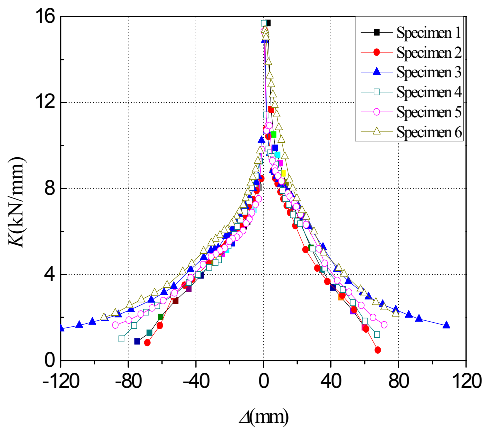

Fig. 7 Stiffness degradation of the specimen

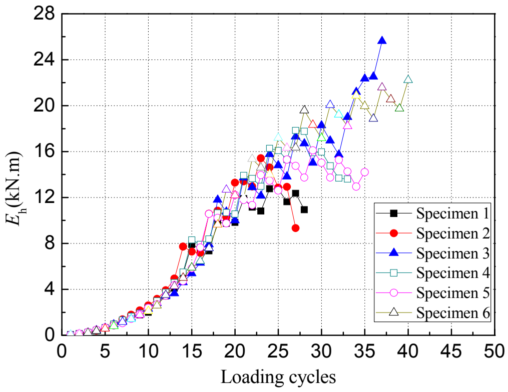

Fig. 8 Energy dissipation curves of the specimen

possible. It is found that the stiffness decreases sharply in the early stage, and then the slope of the stiffness decrease in the later stage. Though the initial stiffness of the six specimens in the forward or the reverse lateral load are almost the same, the stiffness of Specimens 2, 1 and 4 decrease faster than the others, which is reasonable because the cracking and crush of the concrete on and under the beam flange decrease the stiffness of the joint. When cracks appear, the stiffness reduces to less than 60% of its initial value. And the ultimate stiffness, when the strength reduced to 85% of the peak strength, is about 15% of the initial value. The properties described above show that the influence of RCS joint details on the stiffness degradation is not as obvious as that on strength degradation or strength and deformation capacity.

3.7 Energy dissipation capacity

Energy dissipation capacity E_h, which is calculated as the area enclosed by a hysteresis loop, is commonly used to quantify the seismic energy absorption ability of structures. The energy dissipations corresponding to the loading cycle of the six specimens are shown in Fig. 8. Fig. 8 shows that the energy dissipation of the six joints are almost the same in the early stage (before 12 cycle), however with the increase of the loading cycle, the energy dissipation curves differ very much. The energy dissipation of Specimens 1 and 2 are lower than the others, while that of Specimens 3 and 6 are the highest two and Specimens 4 and 5 are in the middle level. This indicates that the band plates in Specimen 3 and the end plates in Specimen 6 can enhance the energy dissipation capacity of the joint much effectively. While the improvement by the joint details in the other specimen are not so obvious.

Equivalent viscous damping coefficient (h_e), which can be calculated by the hysteresis loop areas divided by 2π and the areas of the corresponding triangle at each loading cycle, is another important indicator to evaluate the seismic performance of a structure. The coefficient of the six specimens are 0.263, 0.299, 0.260, 0.286, 0.264, and 0.266, respectively. It is about twice to three times as that of RC joint, which generally is about 0.1. And it is almost the same as the Steel Reinforced Concrete (SRC) joint, which is about 0.3 in general. This indicates that the energy dissipation capacity of the RCS joint is much higher than RC joints and not lower than SRC joints.

4. Conclusions

The six composite RCS joints tested in this investigation showed good seismic performance with stable load versus displacement response, excellent strength and deformation capacity, and good energy dissipation capacity. Two typical failure modes may occur in RCS joints with different joint details. And only minor to moderate joint damage was observed even at the fourth or fifth displacement cycles. End plates, band plates and X shape reinforcement have much effect on the strength capacity of the joint. The increase rate, comparing to the basic specimen is about 30%, 27% and 16%, respectively. The hysteretic behavior and drift capacity of the six specimens also indicate that the joint details used in the research are suitable to resist the earthquake action. The average displacement ductility coefficient of each specimen is larger than 2.0, especially for Specimen 3, it is close to 4.0. The equivalent viscous damping coefficient of the RCS joint are larger than that of RC joint or the same as SRC joints in general. All these seismic behaviors show that the composite RCS joint, assembled with proper joint details, can meet the requirement for earthquake resistant structures.

5. Suggestions

Composite RCS joints with end plate, steel band plate, X shape reinforcement and cover plate could be used in earthquake resistant structures, even in zones of high seismicity, for their excellent strength, deformation capacity and energy dissipation capacity. RCS joints only with face bearing plate, or transverse beam should be designed to prevent the crush of concrete when they are used for earthquake resistant structures.

Two ways can be taken to reduce or prevent the crush of concrete close to the end of columns. One way is to calculate the vertical bearing strength of the joint to make it larger than the vertical bearing forces on the joint, which are mainly caused by the moments and shears transferred between the beam and column. Hence the strength of concrete, the area of bearing zone close to the end of columns, the strength and area of vertical joint reinforcement are key parameters to enhance the vertical bearing strength of the joint. The strength expression can be referred in ASCE (1994). The other way is to add some details in the column. For example, several layer of ties could be provided above and below the beam. In addition, vertical rods, steel angles, or other elements could be attached directly to the steel beam to transfer vertical forces into the concrete column.

The horizontal shear strength of the joint should be the sum of the shear resistance of the steel panel, the joint stirrup and the joint concrete. The contribution of joint details could be taken into account by improving the strength of joint concrete. The mechanical behavior, the mechanical model and the shear strength expressions of the RCS joint would be deduced in the future work.

Acknowledgments

The research described in this paper was financially supported by the National Natural Science Foundation of China (51008244, 51178380) and Natural Science Basic Research Plan in Shaanxi Province of China (2014JQ7245, 2014KJXX-67, 2015JM5173). The authors are grateful for their support. They also thank Dr. T. Schumacher of University of Delaware for his suggestion and feedback in the English writing.

References

ASCE Task Committee on Design Criteria for Composite Structures in Steel and Concrete (1994), "Guidelines for design of joints between steel beams and reinforced concrete columns", *J. Struct. Eng.*, *ASCE*, **120**(8), 2330-2357.

Bahman, F.A., Hosein, G. and Nima, T. (2013), "Seismic performance of composite RCS special moment frames", KSCE *J. Civil Eng.*, **17**(2), 450-457.

Chen, C.H., Cordova, P., Lai, W.C., Deierlein, G.G. and Tsai, K.C. (2004), "Pseudo-dynamic test of full-scale RCS frame. I: Design, construction and testing", *Proceedings of the 13th World Conference on Earthquake Engineering*, Vancouver, Canada, August.

Chou, C.C. and Wu, C.C. (2007), "Performance evaluation of steel reduced flange plate moment connections", *Earthq. Eng. Struct. Dyn.*, **36**(14), 2083-2097.

Chou, C.C. and Chen, J.H. (2010), "Tests and analyses of a full-scale post-tensioned RCS frame subassembly", *J. Construct. Steel Res.*, **66**(11), 1354-1365.

Chou, C.C., Wang, C.Y. and Chen, J.H. (2008), "Seismic design and behavior of post-tensioned connections including effects of a composite slab", *Eng. Struct.*, **30**, 3014-3023.

Cordova, P., Lai, W.C., Chen, C.H. and Tsai, K.C. (2004), "Pseudo-dynamic test of full-scale RCS frame. II: Analyses and design implication", *Proceedings of the 13th World Conference on Earthquake Engineering*, Vancouver, Canada, August.

Deierlein, G.G. and Noguchi, H. (2004), "Overview of U.S.-Japan research on seismic design of composite reinforced concrete and steel moment frame", *J. Struct. Eng.*, *ASCE*, **130**(2), 361-367.

Fargier-Gabaldón, L.B. and Parra-Montesinos, G.J. (2006), "Behavior of reinforced concrete column-steel beam roof level T-connections under displacement reversals", *J. Struct. Eng.*, *ASCE*, **132**(7), 1041-1051.

Griffis, L.G. (1986), "Some design considerations for composite-frame structures", *Eng. J.*, AISC Second Quarter, 59-64.

Guo, Z.X., Zhu, Q.Y. and Liu, Y. (2012), "Experimental study on seismic behaviors of a new type of prefabricated RCS frame connections", *J. Build. Struct.*, **33**(7), 98-105. [In Chinese]

Hiroshi, K. and Isao, N. (2004), "Seismic performance and stress transferring mechanism of through-column-type joints for composite reinforced concrete and steel frames", *J. Struct. Eng.*, *ASCE*, **130**(2), 352-360.

Liang, X.M. and Parra-Moniesinos, G.J. (2004), "Seismic behavior of reinforced concrete column-steel beam subassemblies and frame systems", *J. Struct. Eng.*, *ASCE* **130**(2), 310-319.

Michael, N.B., Joseph, M.B. and Walter, P.M.J. (2000), "Seismic behavior of composite RCS frame systems", *J. Struct. Eng*, *ASCE*, **126**(4), 429-436.

Sheikh, T.M., Deierlein, G.G., Yura, J.A. and Jirsa, J.O. (1989), "Beam-column moment connections for composite frames: Part 1", *J. Struct. Eng.*, *ASCE*, **115**(11), 2858-2876.

CC